

Direct Measurement of the Intermolecular Forces Confining a Single Molecule in an Entangled Polymer Solution

Rae M. Robertson and Douglas E. Smith

Physics Department, University of California, San Diego, 9500 Gilman Dr. La Jolla, California 92093-0379, USA

(Received 22 June 2007; published 21 September 2007)

We use optical tweezers to directly measure the intermolecular forces acting on a single polymer imposed by surrounding entangled polymers (115 kbp DNA, 1 mg/ml). A tubelike confining field was measured in accord with the key assumption of reptation models. A time-dependent harmonic potential opposed transverse displacement, in accord with recent simulation findings. A tube radius of $0.8 \mu\text{m}$ was determined, close to the predicted value ($0.5 \mu\text{m}$). Three relaxation modes (~ 0.4 , 5, and 34 s) were measured following transverse displacement, consistent with predicted relaxation mechanisms.

DOI: [10.1103/PhysRevLett.99.126001](https://doi.org/10.1103/PhysRevLett.99.126001)

PACS numbers: 83.10.Kn, 61.25.Hq, 82.35.Lr

Over the past several decades much effort has been directed at understanding the physical properties of entangled polymer solutions and melts. The reptation theory introduced by de Gennes and extended by Doi and Edwards and others has proven quite successful in describing many experimental findings [1–4]. The key assumption of the theory is that on short time scales each molecule is confined, due to entanglements with surrounding molecules, to move within a tubelike region parallel to its own contour. Motion transverse to the molecular contour is predicted to be highly restricted compared with parallel motion. The advantage of the tube model is that it reduces a complex many-body problem to that of a single polymer moving in an effective mean field. While originally developed for melts, tube models have been successfully extended to polymer solutions using “blob” theory [1,5], in which each chain is divided into correlation blobs of length ζ . The solution is modeled as a melt of chains with monomer size ζ [6].

While tube theories have proven quite useful, the notion of a “tubelike constraint” has remained rather qualitative. No experiment has directly measured the intermolecular forces acting on a single entangled polymer. An expression for the tube radius has been predicted theoretically [2,7], but in practice it has only been defined empirically via measurements of the plateau modulus [2,8]. Thus, the confining tube is present in most theories as an assumption rather than being derived from fundamental molecular properties. Elucidation of the nature of this entanglement field has been identified as one of the primary open challenges in the field [4]. Recently, Zhou and Larson have presented a theoretical method for directly calculating the tube potential via molecular dynamics simulations [9].

In previous work, we directly observed tubelike motion of single entangled DNA molecules by fluorescence microscopy [10,11]; however, we did not quantify the confining forces. A simple picture of the confining potential would be a “hard-walled” square well of radius a . However, individual entanglements certainly lie at dis-

tances smaller and larger than a , and the surrounding polymers are able to reptate, stretch, and deform, causing individual constraints to constantly disappear, reappear, and change locations [4,12]. Zhou and Larson predict that the tube radius actually increases gradually with time [9].

Behavior consistent with predictions of tube models has been observed in rheology experiments and these data have been analyzed to infer properties of the tube [2,4]. For example, when a polymeric fluid is sheared, polymers are stretched and experience elastic and orientational stress. In the Doi-Edwards model (D-E), the stress on the polymer relaxes as it and the surrounding polymers return to equilibrium. At short times, or for small displacements, elastic relaxation is predicted to dominate, with the relevant time scale being the Rouse time τ_R . For $t > \tau_R$ the polymers are predicted to relax by reptation on time scales up to the disengagement time τ_D . Relaxation times have been measured in many rheology experiments but agreement with theory is not always good. Many efforts have been made to improve the theory by introducing various corrections such as contour length fluctuations, residual stretch relaxation, convective constraint release, etc. [2,4,12–14].

Here, we introduce a new experimental approach in which the forces imposed by entangled polymers to confine a single stretched DNA molecule are measured directly using optical tweezers [10,15]. We determine the form of the potential energy landscape restricting molecular displacement. We also characterize the time dependence of the forces by studying the dependence on displacement rate and the relaxation following displacement.

The probe molecule was a 25.3 kbp ($8.4 \mu\text{m}$) DNA prepared as described [16]. It was embedded in a 1 mg/ml ($\sim 40\times$ the overlap concentration c^* [17,18]) solution of linear 115 kbp ($38 \mu\text{m}$) DNA, prepared as described [17]. Previous experiments confirm that we are in the well-entangled regime [8,10].

The probe molecule was attached by each end to optically trapped microspheres (1.1 and $1.4 \mu\text{m}$ radii) and

stretched with an applied tension of 10 pN (fractional extension $\cong 0.95$) as described [16,19] [Figs. 1(a) and 1(b)]. The surrounding molecules were allowed to relax. The optical traps were calibrated as described [19]. 150 mW of laser power was used in each trap, which causes minimal local heating, from $\sim 22^\circ\text{C}$ ambient temperature to $\sim 27^\circ\text{C}$ [20]. To map the confining field, the sample chamber was displaced relative to the trapped probe molecule using a piezoelectric stage. Displacements were made either transverse or parallel to the probe chain contour at constant velocity. The force along the axis of displacement was recorded at 1 kHz and low-pass filtered with a negative-exponential filter (0.1 sampling proportion in a $1\ \mu\text{m}$ range). Measurements were also done without the probe molecule to determine the contribution of the microspheres ($\sim 70\%$), and this force was subtracted from the total force to determine the force acting on the probe molecule. Measurements were repeated $20\times$ at different locations in the sample chamber to verify reproducibility and accurately determine the average induced force.

DNA and numerous synthetic polymer solutions have been shown to exhibit universal rheological properties when scaled according to blob theory [6]. Thus, we chose to scale our measured force by the correlation blob size $\zeta = R_G(c/c^*)^{-\nu/3\nu-1} \cong 52\ \text{nm}$, where R_G is the radius of gyration [1,8,21,22]. We divide the measured force by L/ζ , where L is the probe length, to determine the confining force per blob or unit length.

In traditional D-E theory the tube radius is defined as $a = [24/5(M_e/M)R_G^2]^{1/2}$, where $M_e = (4/5)cRT/G_N^{(0)}$ is the molecular weight between entanglements, M is the molecular weight, and $G_N^{(0)}$ the plateau modulus [2]. Based on previous measurements of $G_N^{(0)}$ for entangled DNA [8,23], and the prediction that $G_N^{(0)}$ is independent of M and proportional to c^2 [2], we estimate $G_N^{(0)} \cong 0.5\ \text{Pa}$ and calculate $a \cong 0.5\ \mu\text{m}$. The accuracy of a is of course limited by the accuracy of the plateau modulus measurements.

Measurements were made with transverse displacements ranging from zero up to $15.5\ \mu\text{m}$. For large displacements ($\geq 3\ \mu\text{m}$), the possibility of generating responses in the nonlinear or “strong flow” regime make the data difficult to interpret, so we focus most of our attention on analyzing the small displacement data relevant to probing the tube. According to reptation theory thermally diffusing chain segments reach the tube radius on the time scale of the equilibration time $\tau_e = a^4/24D_G R_G^2 = 0.02\ \text{s}$ [2,8,21,22,24]. Thus, the characteristic rate at which chain segments are predicted to move a distance a via thermal motion is $a/\tau_e = 25\ \mu\text{m/s}$. Therefore, we made displacements at $25\ \mu\text{m/s}$ in addition to a range of higher and lower rates (0.01 to $65\ \mu\text{m/s}$).

For small displacements the force increased linearly with distance [Fig. 1(d)]. The effective spring constant increased with increasing velocity. In contrast, negligible forces were induced in response to parallel displacements

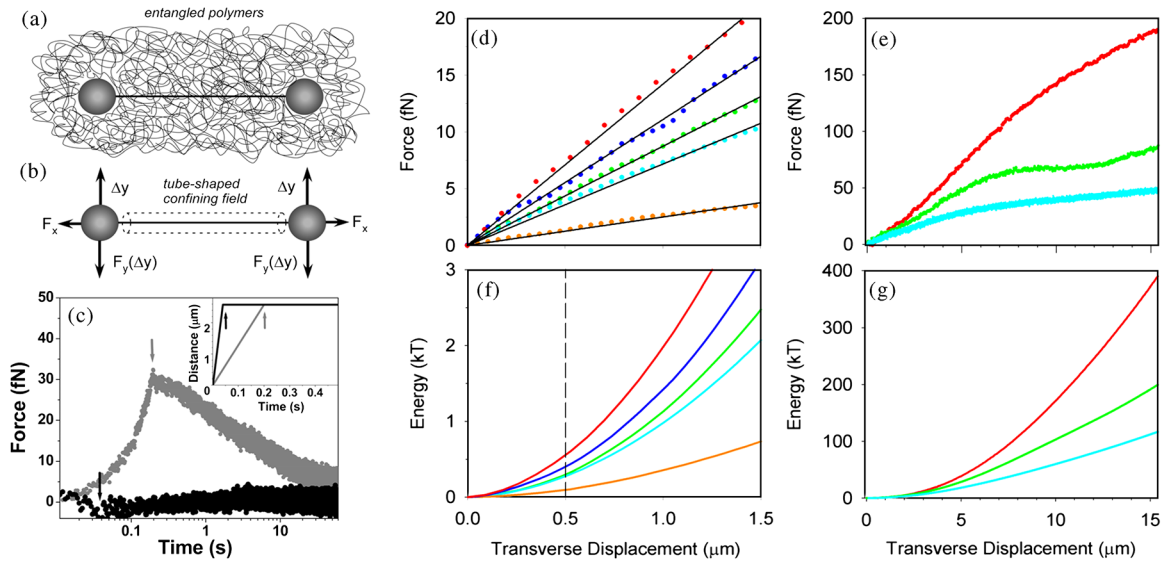


FIG. 1 (color online). (a) Schematic diagram of experiment. A single DNA molecule is held stretched between two optically trapped microspheres and suspended in a concentrated solution of entangled DNA. (b) Reptation models postulate that collective intermolecular interactions give rise to a tubelike confining field (dashed lines). We measure the confining force per unit length (F_x and F_y) in response to an imposed displacement Δx or Δy (see text). (c) Average force induced by a displacement Δy at $13\ \mu\text{m/s}$ (gray) vs a displacement Δx at $65\ \mu\text{m/s}$ (black). Arrows mark the maximum displacements. The inset graph shows the displacement profiles. (d) F_y vs Δy at rates of $65\ \mu\text{m/s}$ (red), $25\ \mu\text{m/s}$ (blue), $13\ \mu\text{m/s}$ (green), $0.52\ \mu\text{m/s}$ (cyan), and $0.10\ \mu\text{m/s}$ (orange). (e) Results for $\Delta y = 15.5\ \mu\text{m}$. (f) Confining potential per unit length $U(y)$ determined by integration of force data in plot (d). The dashed line indicates the theoretically predicted tube radius. (g) $U(y)$ determined by integration of force data in plot (e).

[Fig. 1(c)]. A potential concern with parallel displacements is that the microsphere may partly disturb the surrounding chains through which the probe moves. However, the maximum displacement of $2.6 \mu\text{m}$ was much shorter than the $8.4 \mu\text{m}$ length of the probe molecule so $\sim 70\%$ of the probe was moving through surrounding chains that were undisturbed yet the force was negligible. Thus, we have shown by direct measurement that the collective intermolecular forces imposed by entangled polymers give rise to a tube-shaped confining field. By integrating the perpendicular force vs displacement we can determine the transverse confining potential per unit length $U(y)$ [Figs. 1(f) and 1(g)].

Zhou and Larson [9] calculated $U(y)$ in simulations by determining the relative probability $P(y)$ that a monomer fluctuates a certain transverse distance y from the primitive path and using the relationship $P(y) = e^{-U(y)/kT}$. Although quantitative comparison with our results is not warranted because they simulated a melt rather than a solution, our findings are in qualitative agreement, as expected from blob theory. They find a time-dependent harmonic potential for short times, in accord with our findings. They also find that the tube radius calculated by conventional theory is similar to the characteristic length at which $U(y) \cong kT$ ($P(y) \cong 1/e$) at time τ_e . Similarly, at the relevant $a/\tau_e \cong 25 \mu\text{m/s}$ rate, we find $U = kT$ at $\sim 0.8 \mu\text{m}$, similar to the theoretically predicted tube radius ($0.5 \mu\text{m}$) (Fig. 2).

While the conventional tube model assumes that the tube radius is time-independent, our measurements and recent simulations find a time-dependence [9]. Zhou and Larson have suggested that this effect can help to explain certain long-standing discrepancies between rheological data and theory. They calculate that the tube radius increases by

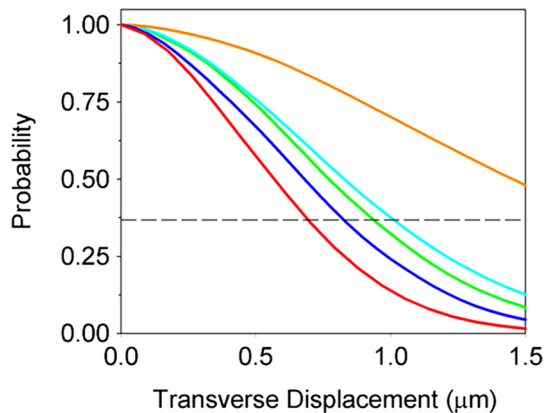


FIG. 2 (color online). Relative probability for a transverse displacement y from the primitive path determined by $P(y) = e^{-U(y)/kT}$, where $U(y)$ is the confining potential [Fig. 1(f)]. Colors indicate displacement rates as in Fig. 1. Tube radius defined as the distance where $P(y) = 1/e$, indicated by the dashed line. Measured tube radii are: $0.65, 0.82, 0.94, 1.0,$ and $1.8 \mu\text{m}$ for the $65 \mu\text{m/s}, 25 \mu\text{m/s}$ (a/τ_e), $13 \mu\text{m/s}$, $0.52 \mu\text{m/s}$, and $0.10 \mu\text{m/s}$, respectively.

$\sim 10\%$ on a time ranging from τ_e to $100\tau_e$. Similarly, our measured tube radius increases by $\sim 20\%$ with displacement rate decreasing from a/τ_e to $a/50\tau_e$.

The longest predicted relaxation time in D-E theory is the disengagement time $\tau_D = (18R_G^2/a^2)\tau_R \cong 40 \text{ s}$, which is the time it takes a chain to completely diffuse out of its initial tube by reptation. On long times approaching τ_D we expect the tube constraints to weaken and eventually disappear. Indeed, at the lowest displacement rate in our experiment ($0.1 \mu\text{m/s}$), corresponding to $\sim 10a/\tau_D$, we find a potential of only $0.2kT$ at the $0.8 \mu\text{m}$ tube radius. It rises to $\sim kT$ at $\sim 2 \mu\text{m}$, indicating ineffective tube confinement.

Our results for large displacements may be more difficult to interpret, as discussed above. We nevertheless present these findings [Figs. 1(e) and 1(g)], since the tube model has been applied in many cases to nonlinear states generated by strong flows [2,4]. For all three rates a decrease in dF/dy was observed for $\Delta y > 7 \mu\text{m}$, which is close to the predicted equilibrium primitive path length of the entangled DNA [$L_0 \cong (M/M_e)a \cong 9 \mu\text{m}$] [2]. This decrease may indicate displacement-induced slippage of entanglements off of the probe molecule. Such behavior may be related to that proposed to occur in ‘‘convective constraint release’’ models for nonlinear responses in shear flow [8].

Further information came from the measured force relaxation following the displacements (Fig. 3). Inverse Laplace transform analysis revealed three distinct decay times for all data sets except the $0.1 \mu\text{m/s}$ case where only the two faster relaxation times were observed. The time constants and amplitudes were insensitive to the displace-

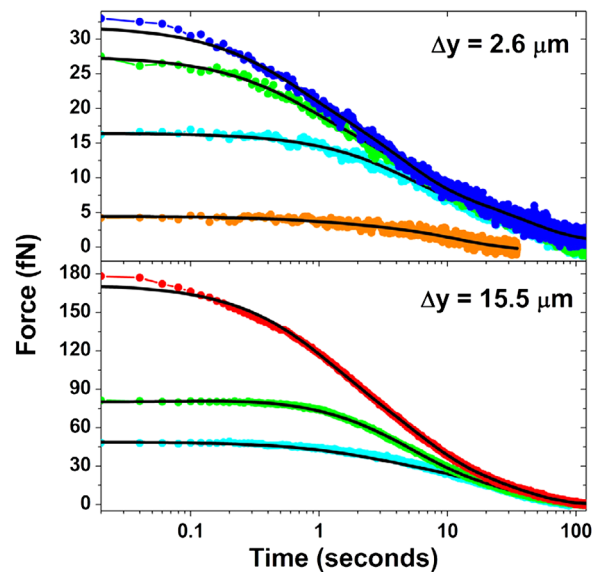


FIG. 3 (color online). Force relaxation following transverse displacements of 2.6 or $15.5 \mu\text{m}$. Colors indicate displacement rates as in Fig. 1. The solid lines are fits to sums of decaying exponentials (see text).

ment rate and size. To accurately determine the time constants the averaged relaxation curves were fitted to a discrete sum of three decaying exponentials, yielding $\tau_1 = 0.45 \pm 0.34$ s, $\tau_2 = 5.4 \pm 2.8$ s, and $\tau_3 = 34 \pm 5.8$ s. The relative amplitudes of these decay components were all roughly equal (each $\sim 1/3$ of the total).

These measurements probe the relaxation of the distorted molecules surrounding the probe molecule. According to D-E theory [2], the shortest relaxation time is the Rouse time $\tau_R = 6R_G^2/3\pi^2 D_G$ over which a deformed polymer elastically relaxes back to L_0 . We calculate $\tau_R = 0.6$ s [8,21,22], in good agreement with our measured τ_1 . Theory also predicts that elastic relaxation accounts for only 1/5 of the total relaxation, attributing 4/5 to disengagement from the tube [25]. However, we find a $\sim 1/3$ contribution for τ_1 . It is possible that this larger amplitude is due to the contribution of unresolved higher order Rouse modes to τ_1 [25].

The longest predicted relaxation time, the disengagement time $\tau_D = 40$ s, is consistent with our measured value of τ_3 . Its 1/3 contribution is much lower than the predicted 4/5, however, we find a distinct intermediate decay time $\tau_2 = 12\tau_1$, not predicted by D-E theory, that also contributes, suggesting that reptation is occurring on this intermediate time scale τ_2 as well. A similar relaxation time was recently observed in nonlinear step shear experiments with polystyrene solutions [13,26] and in flow deformation studies of DNA at $35c^*$ [8]. Mhetar and Archer have proposed an explanation for this relaxation mode [14]. They propose that the tube diameter shrinks during deformation, as its length is increased, prohibiting complete relaxation of chain extension to L_0 in time τ_R . An intermediate relaxation mode arises when the residual stretch relaxes as the tube expands back to its equilibrium diameter. Reptation is also predicted to occur on this time scale; however, complete disengagement from the tube only occurs after a time τ_D . While the nature of the deformation of the entangled polymers was different in the previous flow experiments than in our experiment, in both cases entangled polymers were deformed and allowed to relax. Our findings suggest that the relaxation mechanism proposed by Mhetar and Archer, which is the only model to our knowledge that proposes such an intermediate relaxation time, may apply in both cases.

Finally, we examine the dependence of the confining force on length and concentration of the surrounding chains. We made additional measurements using shorter 11 kbp DNA at 1 mg/ml ($\sim 7.5c^*$, $\zeta \cong 50$ nm) and 115 kbp DNA diluted to 0.1 mg/ml ($\sim 4c^*$, $\zeta \cong 300$ nm). The measured forces were similar for both cases and significantly lower than that for the 115 kbp, 1 mg/ml solution. With the most extreme deformation (15.5 μm at 65 $\mu\text{m/s}$) the maximum force was only ~ 50 fN for both cases compared with ~ 200 fN for the 115 kbp, 1 mg/ml solution. Also, both relaxations were well described by

only a single time constant of ~ 0.5 s, which is close to the predicted value of τ_R . These findings suggest that at these lower concentrations and lengths the molecules are not yet entangled so there is no effective confining tube.

We thank R. Larson, A. Schweizer, P. Rickgauer, and D. Fuller for assistance and the Petroleum Research Fund, Sloan Foundation, and NSF for support.

-
- [1] P.G. de Gennes, *Scaling Concepts in Polymer Physics* (Cornell University, Ithaca, 1979).
 - [2] M. Doi and S.F. Edwards, *The Theory of Polymer Dynamics* (Oxford, New York, 1986).
 - [3] R.G. Larson, *The Structure and Rheology of Complex Fluids* (Oxford, New York, 1998).
 - [4] T.C.B. McLeish, *Adv. Phys.* **51**, 1379 (2002).
 - [5] R.H. Colby and M. Rubinstein, *Macromolecules* **23**, 2753 (1990).
 - [6] Y. Heo and R.G. Larson, *J. Rheol.* **49**, 1117 (2005).
 - [7] K. Kremer and G.S. Grest, *J. Chem. Phys.* **92**, 5057 (1990).
 - [8] R.E. Teixeira, A.K. Dambal, and D.H. Richter *et al.*, *Macromolecules* **40**, 2461 (2007).
 - [9] Q. Zhou and R.G. Larson, *Macromolecules* **39**, 6737 (2006).
 - [10] T.T. Perkins, D.E. Smith, and S. Chu, *Science* **264**, 819 (1994).
 - [11] D.E. Smith, T.T. Perkins, and S. Chu, *Phys. Rev. Lett.* **75**, 4146 (1995).
 - [12] J.P. Montfort, G. Marin, and P. Monge, *Macromolecules* **17**, 1551 (1984).
 - [13] L.A. Archer, J. Sanchez-Reyes, and Juliani, *Macromolecules* **35**, 10216 (2002).
 - [14] V. Mhetar and L.A. Archer, *J. Non-Newtonian Fluid Mech.* **81**, 71 (1999).
 - [15] S.B. Smith, Y. Cui, and C. Bustamante, *Science* **271**, 795 (1996).
 - [16] D.N. Fuller, G.J. Gemmen, and J.P. Rickgauer *et al.*, *Nucleic Acids Res.* **34** e15 (2006).
 - [17] S. Laib, R.M. Robertson, and D.E. Smith, *Macromolecules* **39**, 4115 (2006).
 - [18] R.M. Robertson and D.E. Smith, *Macromolecules* **40**, 3373 (2007).
 - [19] J.P. Rickgauer, D.N. Fuller, and D.E. Smith, *Biophys. J.* **91**, 4253 (2006).
 - [20] H. Mao, J.R. Arias-Gonzalez, and S.B. Smith *et al.*, *Biophys. J.* **89**, 1308 (2005).
 - [21] R.M. Robertson, S. Laib, and D.E. Smith, *Proc. Natl. Acad. Sci. U.S.A.* **103**, 7310 (2006).
 - [22] J.S. Hur, E.S.G. Shaqfeh, and H.P. Babcock *et al.*, *J. Rheol. (N.Y.)* **45**, 421 (2001).
 - [23] D. Jary, J.-L. Sikorav, and D. Lairez, *Europhys. Lett.* **46**, 251 (1999).
 - [24] M. Putz, K. Kremer, and G.S. Grest, *Europhys. Lett.* **49**, 735 (2000).
 - [25] A.E. Likhtman and T.C.B. McLeish, *Macromolecules* **35**, 6332 (2002).
 - [26] J. Sanchez-Reyes and L.A. Archer, *Macromolecules* **35**, 5194 (2002).